



X-RAY MICROANALYSIS OF ETOPOSIDE-INDUCED APOPTOSIS IN THE PC-3 PROSTATIC CANCER CELL LINE

M. SALIDO^{1*}, J. VILCHES¹, A. LOPEZ¹ and G. M. ROOMANS²

¹*Department of Cell Biology, School of Medicine, University of Cadiz, Spain*

²*Department of Medical Cell Biology, Uppsala University, Sweden*

Received 3 August 2000; accepted in revised form 30 October 2000

Apoptosis comprises a critical intracellular defense mechanism against tumourigenic growth. We have been interested in the relationship between morphological changes and intracellular concentration of several cations after etoposide-induced apoptosis in androgen-independent prostate cancer cells. SEM and X-ray microanalysis were performed on freeze-dried PC3 cells after etoposide treatment, and correlated with the morphological features observed after examination by light and fluorescence microscopy. Cell viability assays were also performed. A significant decrease in intracellular Cl^- and K^+ and a progressive increase in Mg^{2+} and Na^+ were observed, with parallel changes in cellular volume as cells passed through three morphological stages of apoptosis. The use of EPXRMA made it possible to evaluate alterations in element composition in prostate cancer cell apoptosis and may be a helpful tool for further studies on apoptosis in prostate cancer.

© 2001 Academic Press

KEYWORDS: electron probe X-ray microanalysis; intracellular ions; apoptosis; prostate cancer; androgen-independent; etoposide.

INTRODUCTION

Prostatic cancer is the most commonly diagnosed neoplasm and the second leading cause of male death. According to the kinetics of tumour growth, an increase in a neoplastic cell population is the result of the imbalance between the two processes controlling tissue homeostasis: cell proliferation and cell death. Apoptosis therefore comprises a critical intrinsic cellular defense mechanism against tumourigenic growth which, when suppressed, may contribute to malignant development (Kerr *et al.*, 1994). Multiple genetic and epigenetic factors have been implicated in the oncogenesis and progression of prostate cancer, but the molecular mechanisms underlying the disease remain largely unknown (Kyprianou, 1994; Tu *et al.*, 1996; Lu *et al.*, 1999; Schwartzman and Cidlowski, 1993; Schwartz and Osborne, 1993). A wide variety of cytotoxic agents with different intracellular targets can induce the

uniform phenotype of apoptosis (Kerr *et al.*, 1972). This implies that the cytotoxic activity of anti-cancer drugs is not solely dependent on specific drug-target interactions but also on the activity of an apoptotic machinery (Denmeade and Isaacs, 1996; Berges *et al.*, 1993; Kawamura *et al.*, 1996; Kyprianou *et al.*, 1990; Borner *et al.*, 1995; Frost *et al.*, 1999).

Recent studies have suggested a primary role for intracellular ions, especially potassium (K^+), in the activation of caspases implicated in apoptosis (Hughes *et al.*, 1997), and K^+ loss seems to be crucial for the activation of endonucleases in intact cells (Dallaporta *et al.*, 1998). Sustained elevations in intracellular calcium are known to be related to the process (Furuya *et al.*, 1994; Zhu and Wang, 1999). Recently chloride has also been implicated in apoptosis (Szabo *et al.*, 1998; Fujita *et al.*, 1997). Apoptotic cells pass through morphologically identifiable changes in their pathway to death, with loss of cellular volume and cell shrinkage, while nuclei shrink until complete disintegration of the cell into apoptotic bodies occurs (Kerr *et al.*, 1994;

*To whom correspondence should be addressed: Dr Mercedes Salido, Department of Cell Biology, School of Medicine, University of Cadiz, Plaza Fragela s/n 11003 Cádiz, Spain. E-mail: mercedes.salido@uca.es

Earnshaw, 1995). Alterations in cell volume are accompanied by the movement of water across the cell membrane and activation of volume-regulated ion transport channels, mainly K^+ and Na^+ (Beauvais *et al.*, 1995; McCarthy and Carter, 1997).

Electron probe X-ray microanalysis has been used for the last 25 years by biologists to obtain information about the distribution of elements at the cell and tissue level. During this period, progress has mainly been made through the development of more adequate techniques for specimen preparation (mainly low temperature techniques) and quantitative analysis of physiologically important cellular ions (Roomans, 1990; Roomans and von Euler, 1996; Elder *et al.*, 1998; Hongpaisan *et al.*, 1996). X-ray microanalysis can be used to study the distribution of elements in prostatic cells lines at the cellular and subcellular levels in a variety of physiological and pathophysiological conditions (Halgunset *et al.*, 1992).

Electron probe X-ray microanalysis is unique because it combines the ability to undertake chemical analysis with the high resolution of the electron microscope and thus is capable of correlating chemical information with known ultrastructural details. Microprobe analytical techniques take advantage of the physical interactions that occur when an electron beam impinges on a specimen. One such interaction is the production of X-rays with energy and wavelength characteristics indicative of the elemental composition of the specimen interacting with the electron beam (Warley, 1997; Ingram *et al.*, 1999). Use of *in vitro* systems and cell cultures may further increase the number of problems to which X-ray microanalysis can be applied. Among the numerous applications of X-ray microanalysis in cell biology and cell pathology, the role of ions in programmed cell death is of interest (Skepper *et al.*, 1998; Bowen *et al.*, 1988).

We have been interested in the cellular concentration and distribution of several cations in the androgen-independent prostate cancer cell line PC-3, and their relationship with programmed cell death in these cells. We wanted to assess the degree of induced apoptosis in neoplastic prostate cell lines in culture by comparing microanalytical data with those obtained after examination of apoptotic cells by light and fluorescence microscopy (Salido *et al.*, 1996; Salido *et al.*, 1999). In addition we wanted to describe the different phases of etoposide-induced programmed cell death in these cells and their correlation with morphology as assessed by scanning electron microscopy. This may be useful in future studies

and could contribute to a better understanding of the apoptotic process in prostatic epithelium (Schwartzman and Cidlowski, 1993; McConkey, 1996; Kawamura *et al.*, 1996; Gschwend, 1996).

MATERIALS AND METHODS

The androgen-independent cell line PC-3, a p53 deficient prostate cell line derived from a bone metastasis (Nuclear Iberica, Madrid, Spain), was used for this study. Cells were grown in Dulbecco's Modified Essential Medium (DMEM) (ICN Biomedicals, Aurora, Ohio, U.S.A.) supplemented with 10% Foetal Bovine Serum (FBS) (Serva, Heidelberg, Germany), 4% penicillin-streptomycin (Biochrom, Berlin, Germany) and 0.4% gentamycin (Gibco, Paisley, Scotland, UK) under standard conditions, in a water saturated atmosphere of 5% CO_2 until the experiment was started.

The cell lines used were authenticated by the source, checked at regular intervals, as also for contamination, and used at low passage number, in accordance with the UKCCCR guidelines.

Treatment protocols

All experiments were started with unsynchronised exponentially growing cultures. Cells were seeded in microplates (Nunclon, Madrid, Spain) at a density of 100,000 cells/ml in each well. Culture media supplemented with 5% FBS, 4% penicillin and 0.4% gentamycin were added and 48 h later changed (t_0) to medium with etoposide (Sigma, St Louis, Missouri, U.S.A.) added (from a 2 mM stock solution in DMSO) at doses of 80 μ g/ml, 100 μ g/ml, and 150 μ g/ml. In the control only culture medium was added. The cells were examined after 0, 24 and 48 h of treatment.

Cell parameter analysis

Direct examination by phase-contrast microscopy. With a Nikon Diaphot phase contrast microscope adapted with a photographic system, we could observe morphological changes such as cell surface alterations, blebbing, detachment and rounding of treated cells.

Growth kinetics and cell viability. Determined by XTT viability assay and trypan blue exclusion, with trypan blue in the culture medium (0.5% v/v). After incubation of cells with trypan blue, and

observation in a haematocytometer, non-stained cells are regarded as viable, and blue cells are considered non-viable.

Percentage of viable cells. (Number of non stained cells/total cell number) \times 100.

XTT assay. (Boehringer Mannheim, cat. no. 1465015). Briefly, cells were grown in a microtiter plate, 96 wells, flat bottom, in a final volume of 100 μ l culture medium per well, in a humidified atmosphere (37°C and 5% CO₂), during the assay. After 24 and 48 h, 50 μ l of the XTT labelling mixture was added to each well. Cells were incubated for 4 h in a humidified atmosphere and absorbance of cells was measured using an ELISA plate reader at a wavelength of 450–500 nm.

Determination of apoptosis. For microscopical quantification of apoptotic cells, we used cytospin preparations obtained from *in vitro* cell cultures. Apoptotic cells round up and detach from the substrate. The sample is taken by collecting the supernatant, containing the floating apoptotic cells, followed by trypsinisation of the rest of the monolayer, containing viable cells. Both fractions were added together to reconstitute the total population and then centrifuged at 1000 rpm for 5 min to obtain the pellet. Cells were then washed twice in PBS and cytospun by means of cytobuckets, at 1500 rpm for 5 min. Samples were air dried and afterwards stained for observation by light and fluorescence microscopy.

Haematoxylin-eosin stain. Air-dried slides were fixed in 10% formaldehyde, stained with haematoxylin and counterstained with eosin.

Apoptosis staining: fluorescent DAPI. Air-dried slides were fixed in methanol (Panreac, Barcelona, Spain) at -20° for 20 min, air dried and stained with 4',6'-diamino-2-phenylindol (DAPI) (Serva) at room temperature and in darkness for 20 min, and mounted with antifading media—O-phenyldiamine (Sigma) in glycerol (Merck, Darmstadt, Germany) and preserved in darkness at -20° C until examination by fluorescence microscopy, at wavelengths between 300 and 400 nm.

Percentage of apoptotic cells. Defined as (number of apoptotic cells/total cell number) \times 100. At least 200 cells were counted for each experiment.

Flow cytometry. Cells (10^5) were centrifuged at 1000 rpm for 5 min, and washed three times in PBS. Pellet was resuspended in 425 μ l PBS and 25 μ l propidium iodide. 50 μ l NP40 in 1% PBS were added, prior to cytometric analysis (Epics XL Coulter).

DNA fragmentation. Samples (10^6) were washed in PBS and resuspended in 50 μ l Tris borate EDTA, pH 8 (Merck), 2.4 μ l Nonidet P40 (Sigma). Then 2 μ l RNase 1/100, 1 mg/ml (Sigma) were added to each sample prior to incubation at 37° for 2 h. Ten microlitres of proteinase K (Boehringer Mannheim) were added and incubation at 37°C continued overnight. Samples were heated to 65°C, and 20 μ l agarose were mixed with each sample before loading them into the dry wells of a 2% agarose gel in TAE 1 \times (Merck). Molecular weight marker was loaded, 4 μ l marker (Amresco E-261), 8 μ l water and 0.25 μ l bromophenol blue in 10 μ l 1% agarose (Pronadisa). Gels were run at 70 V until the marker dye had migrated 3–4 cm, and then at 15 V overnight. DNA was visualized by staining in ethidium bromide and destaining in water.

Mean and SD representative of at least ten experiments are given. ANOVA and a two-tailed Student's *t*-test were performed for statistical validation of the results.

Microanalytical study: specimen preparation and analysis

For scanning electron microscopy and EPXMA cells were seeded onto polycarbonate tissue culture plate well inserts (Millicell-PCF, Millipore, Bedford, MA, U.S.A.), at a density of 50,000 cells/ml, under standard culture conditions as described above and treated according to the previously described protocol (Salido *et al.*, 1999). After treatment, supernatants were also collected on separate polycarbonate filters, in order to collect all detached and undetached cells, and then transferred to conical centrifuge tubes and centrifuged at 170 \times *g* for 3–5 min. Previous studies have shown that polycarbonate membrane filters do not interfere with spectra generated from the cells, and no correction for extraneous background was necessary (Fernández-Segura *et al.*, 1999).

Polycarbonate membrane filters were then cut from their polystyrene holder and washed with ice-cold distilled water for 5 s to remove the culture medium and prevent the extracellular medium from contributing to the intracellular elemental content. This procedure does not interfere with elemental content or morphology of the cells. After washing, specimens were immediately plunge-frozen in

liquid nitrogen (LN₂), and placed in a precooled aluminium specimen holder at LN₂ temperature. The specimen holder was then transferred to an E5300 Polaron freeze drier (Polaron, Watford, U.K.) and cells were freeze dried for 20 h at -50°C and 10⁻¹/mbar vacuum pressure. The membrane filters were then fixed with adhesive graphite lamina onto stubs and coated with carbon in a high vacuum coating system (Hitachi, Tokyo, Japan).

EPXMA was performed on whole freeze-dried PC-3 cells in a Philips XL30 scanning electron microscope. The microscope was equipped with an Si (Li) energy-dispersive X-ray detector (EDAX international). Analytical conditions: tilt angle 35°, take off angle 60°, working distance 10 mm; magnification: ×10,000, cps 450–600. X-ray spectra were acquired at an accelerating voltage of 10 kV, and collected in the static spot mode for 200 s live time. Only one spectrum was acquired from each cell. The concentration of element x in the specimen (C_{xsp}) was obtained with the peak-to-local-background (P/B) ratio method, and was calculated according to the formula

$$C_{xsp} = \frac{(P_x/B_x)_{sp}}{(P_x/B_x)_{std}} \frac{G_{sp}}{G_{std}} C_{xstd}$$

where C_x is the concentration of element x in millimoles per kilogram (dry weight), (P_x/B_x) is the peak to background ratio for the element x, the subscripts sp and std refer to specimen and standard, respectively, and the G value is the mean value of the atomic number squared (Z²) and divided by the atomic weight (A) in the sample. Cellular elemental concentrations were obtained with reference to 20% dextran standards containing known amounts of inorganic salts (Warley, 1990).

Statistical evaluation. Data are presented as the mean ± standard error of the mean (SEM) of at least ten independent experiments. Twenty cells were measured in each analysis. Initial statistical comparison of element concentrations was made using ANOVA. Homogeneity of means was tested using the Bonferroni's test. Student's *t*-test was used to evaluate the statistical significance of the difference between means; a value of *P* < 0.005 was considered statistically significant.

RESULTS

Characterization of the apoptotic process

Scanning electron microscopy of the cultured prostatic cells confirmed the results that we previously

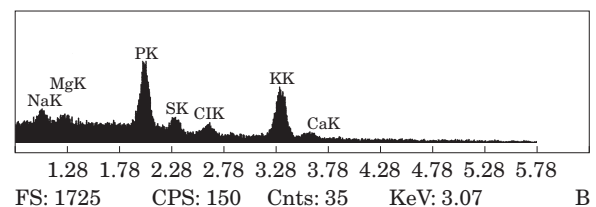
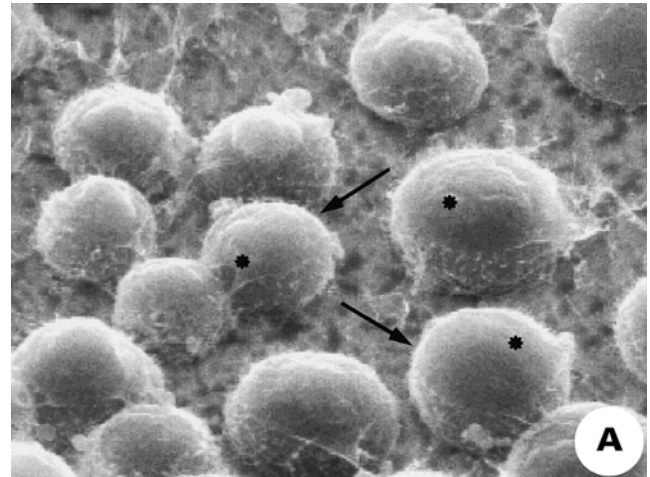


Fig. 1. (A) Scanning electron micrograph of freeze dried control cells (*) that appear to be round with well preserved cytoplasm and plasma membrane and display a smooth surface (†). (B) X-ray spectra of control cells.

obtained with light and fluorescence microscopy (Salido *et al.*, 1999). Briefly, control cells were round with well-preserved cytoplasm and plasma membrane (Fig. 1), and treated cells passed through a series of morphologically identifiable stages in their pathway to death. In the initial phase of the apoptotic process (Fig. 2) cells shrank due to a loss of cytoplasmic volume, became detached from their neighbours and from culture substrata and adopted a smooth contour. In a following phase, the plasma membrane ruffled and blebbed (Fig. 3). In the third phase, progressive degeneration of residual nuclear and cytoplasmic structures was observed (Fig. 4). The micrographs show specimens that were also used for X-ray microanalysis.

Percentages of apoptotic cells

After 48 h of treatment with 100 µg/ml etoposide, the percentage of apoptotic cells according to examination of haematoxylin-eosin and DAPI stained cells was 61.7% in exposed cells and 7.1% in non-treated (control) cells.

Cell cycle distribution and DNA assays

Flow cytometric studies of etoposide-treated cells showed an increase of fluorescence in the sub G₁

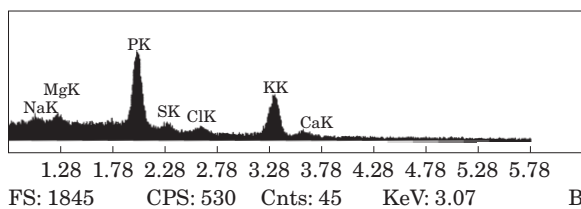
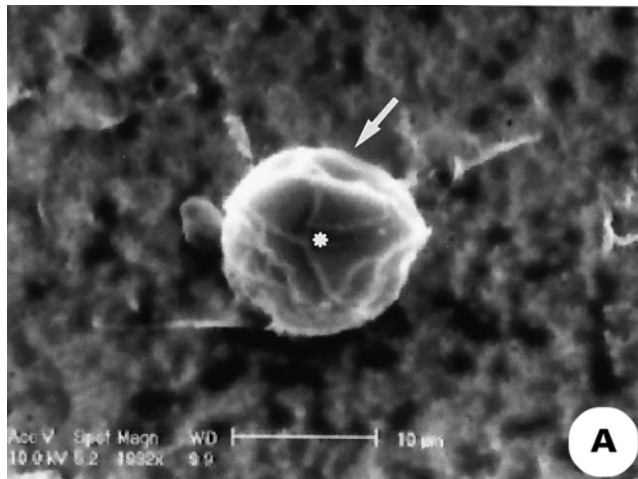


Fig. 2. (A) Etoposide-treated PC-3 cells. (*) In the first stage of the process, cells shrank due to a loss of cytoplasmic volume, because detached from their neighbours and from culture substrata and adopted a smooth contour (↑). (B) X-ray spectra corresponding to first stage of apoptosis in PC3 cells. Note that cells have lower Cl K α and K K α and higher P K α peaks than control cells.

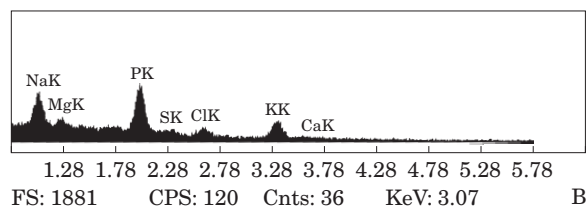
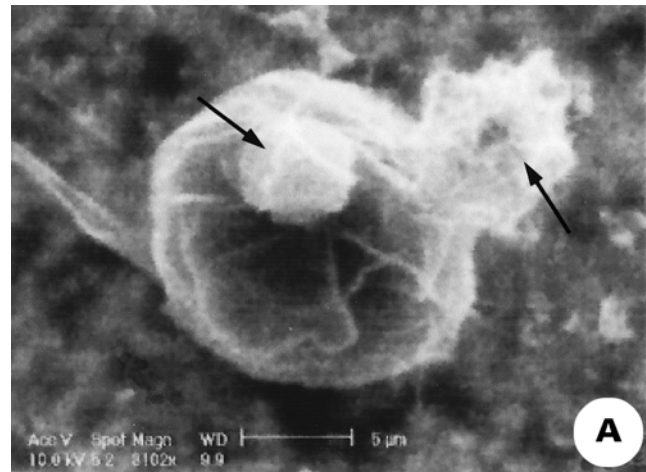


Fig. 3. (A) In the second stage of apoptosis, the plasma membrane of shrunken etoposide treated cells ruffled and blebbed (↑). (B) X-ray spectra in second stage of apoptosis. Na K α and Mg K α peaks progressively increase while Cl K α and K K α peaks decrease when compared to control cells and to previous stage of apoptosis.

region, and also an accumulation of cells in the G₂+M area, in comparison to control cells. When agarose gel electrophoresis was performed for DNA, internucleosomal fragmentation was found in PC-3 treated cells and not in controls.

Growth kinetics and cell viability

Cell viability assessed by trypan blue exclusion dye assay revealed 85.3% viable cells in the control group and 53.1% in the etoposide-treated group. According to the XTT assay, 90% of the cells in the control group and 54% of the treated cells were considered viable.

The percentages of trypan blue-stained cells did not, as expected, correlate exactly with the value of apoptotic cells. In the first stage of apoptosis, the cell membrane did not become permeable to the vital dye as cell integrity was still preserved and only in the final stage did the progressive degeneration of cultured cells cause membrane rupture, making the cells permeable to vital dyes.

Cell damage

Treatment of prostate cancer cells with etoposide caused a significant decrease in the cellular content

of Cl⁻ ($P < 0.0016$) and K⁺ ($P < 0.0001$) and a progressive increase in Mg²⁺ ($P < 0.01$) and Na⁺ ($P < 0.0006$) (Figs 5 and 6). The changes in Na⁺ and K⁺ resulted in a progressively increasing Na/K ratio, significantly different from the control value from stage II onwards ($P < 0.0001$) (Fig. 7). In the first stage of apoptosis a small increase in phosphorus was observed, but in the second stage a small decrease was seen. The concentration of sulphur decreased both in the first and the second stage, and this resulted in a significant increase in the P/S ratio in the first and second stages ($P < 0.001$) (Fig. 7). In the third phase a marked increase in P was seen, accompanied by a substantial increase in Ca²⁺ (Figs 5 and 6).

Volume changes

The variation in cell volume was evaluated from the sum of the Na⁺ and K⁺ content (Fig. 8).

DISCUSSION

A major problem that can be investigated by quantitative X-ray microanalysis of biological material is the sensitivity of living cells to various

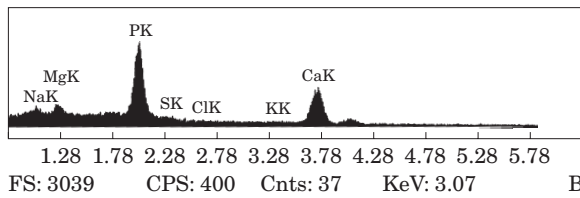
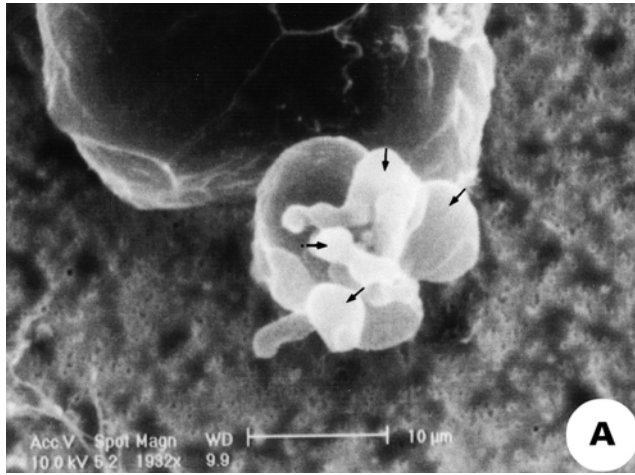


Fig. 4. (A) In the third phase, progressive degeneration of residual nuclear and cytoplasmic structures was observed as cell disintegrates into apoptotic bodies (†) while (B) an increase in P K α and a substantial increase in Ca K α appear in X-ray spectra.

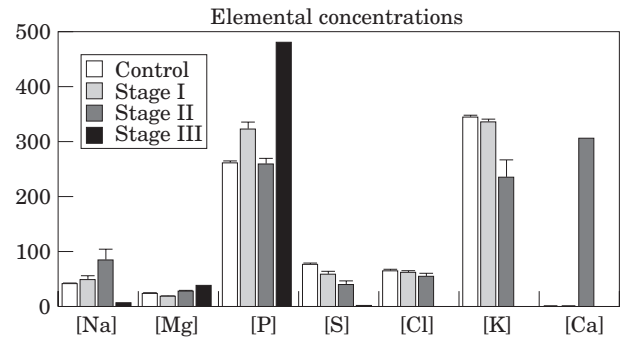


Fig. 6. A significant decrease in the cellular content of Cl ($P < 0.0016$) and K ($P < 0.0001$) and a progressive increase in Mg ($P < 0.01$) and Na ($P < 0.0006$), was found in etoposide-treated cells when compared to control cells.

kinds of harmful changes in their environment causing rapid and marked alterations in the intracellular elemental concentrations (Rodman-Smith and Cameron, 1999; Roomans *et al.*, 1996).

Apoptosis is accompanied by major changes in ion compartmentalisation and transmembrane potentials, with transient mitochondrial swelling and a subsequent loss of plasma membrane potential related to the loss of cytosolic K⁺, cellular shrinkage and DNA fragmentation (Dallaporta *et al.*, 1999). In the present study, we have shown a correlation between morphologically identifiable changes in the androgen-independent prostate

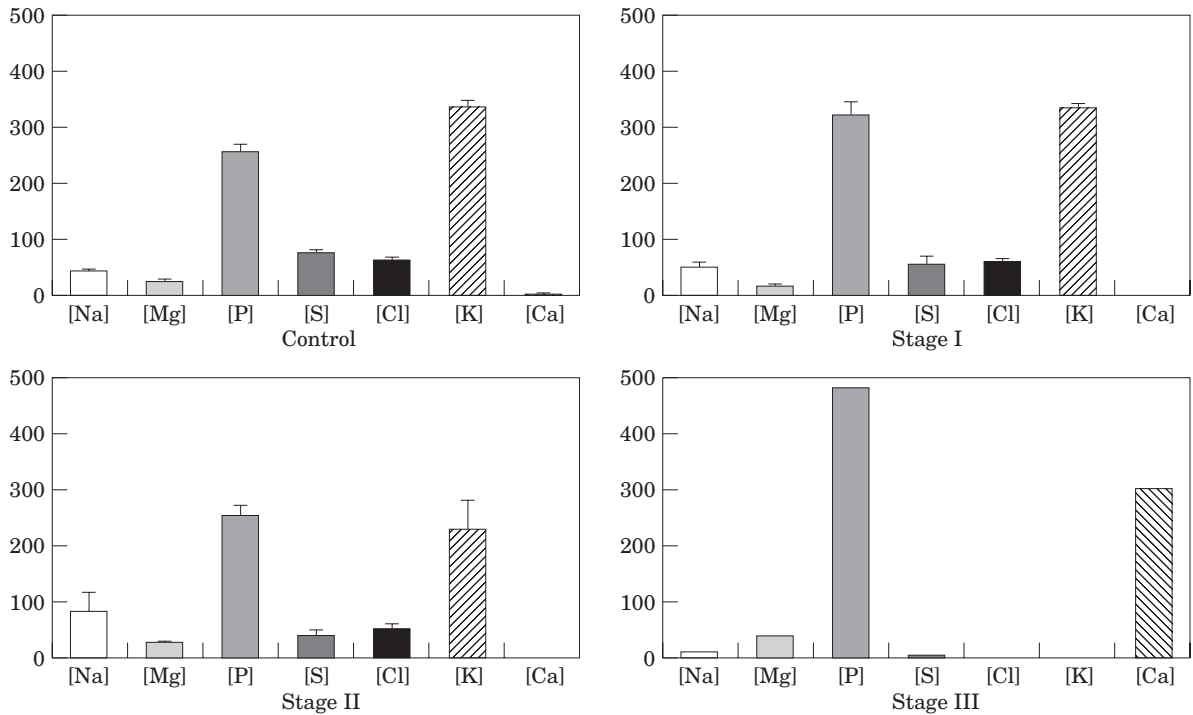


Fig. 5. Elemental content in control and etoposide-treated PC3 cells.

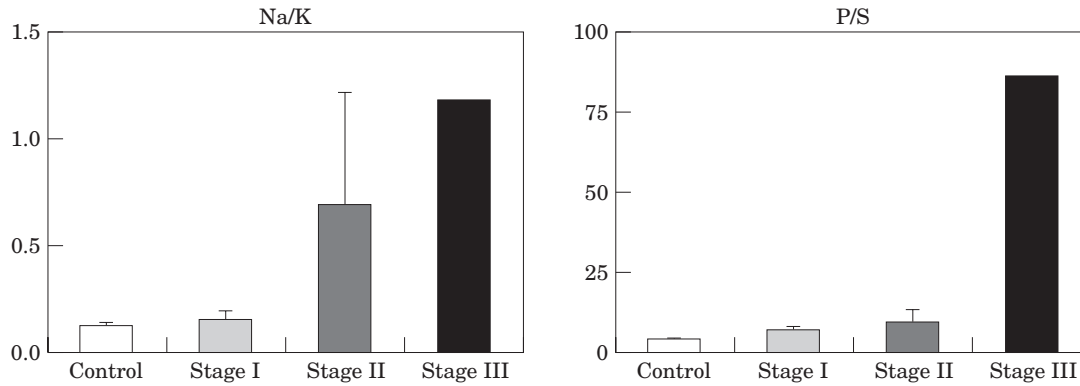


Fig. 7. Na/K and P/S ratios show a progressive and significant ($P < 0.001$ compared to control) increase through the three stages of apoptosis.

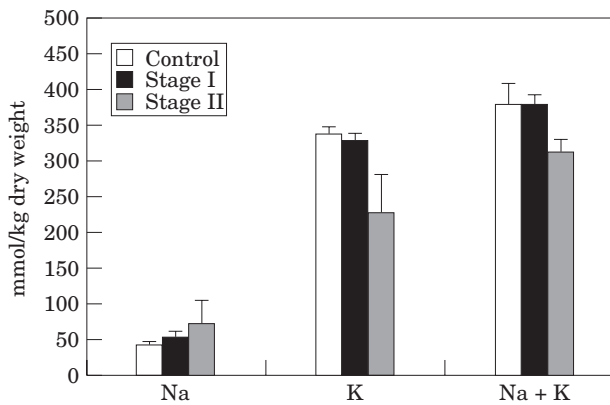


Fig. 8. The shrinkage of the etoposide-treated cells was correlated with microanalytical data where the sum of the Na and K content was used to assess the variation in cell volume.

cancer cell line PC-3 during apoptosis after etoposide treatment and the elemental changes compatible with progressive cell damage (Saraste, 1999; Skepper *et al.*, 1999).

The culture techniques used in the present experiments were designed in order to permit rapid cryofixation of intact cell monolayers for subsequent X-ray microanalysis (Roomans, 1991; Fernandez Segura *et al.*, 1999). When X-ray microanalysis is carried out on cells on a solid substrate, as in the present study, there is a risk that the electron beam overpenetrates the cell, even at low accelerating voltage. To normalise the intensity counts of the different elements with respect to the mass of the cell analysed, the phosphorus intensity signal is often taken as a measure of the analysed mass and as a unit of reference for evaluating the peak intensity of the other elements (Abraham *et al.*, 1985). However, this requires that the P content is constant during the experiment. In a process such as apoptosis that affects cellular macromolecules,

and progresses over a considerable period of time, it may be safer not to make this assumption. However, elemental ratios are insensitive to the problem of overpenetration, and may yield important biological information. Hence, the increase in P/S ratio may be explained as a relative increase of P-containing macromolecules (mainly nucleotides) relative to S-containing macromolecules (mainly proteins). The relative increase in P content matches with the etoposide-induced arrest in G₂/M (Barbiero *et al.*, 1995) which would result in an increased nucleotide content.

Also the increase in Na/K ratio is of physiological significance. The difference in concentrations of Na⁺ and K⁺ over the cell membrane plays a crucial role in cell physiology, and the maintenance of the gradients requires an adequate energy supply, an intact cell membrane and specific enzymatic activities. When the Na⁺/K⁺ pump in the cell membrane lacks energy to maintain the ionic gradients, in the absence of a membrane potential, large amounts of calcium ions flow through the voltage-dependent ion channels, down an extreme extra/intracellular concentration gradient, into the cell (Berger and Garnier, 1999; Sandström *et al.*, 1994; Fujii *et al.*, 1999). Thus, the ratio of intracellular Na⁺ to K⁺ can be used as a very sensitive measure of various kinds of cell injury. Perturbation of the intracellular levels of these two elements can be detected by X-ray microanalysis in cells and tissues undergoing programmed cell death (Bowen *et al.*, 1988; Skepper *et al.*, 1999; Fernandez-Segura *et al.*, 1999).

Shifts in the resting potential of the cell membrane may also result from the activation of specific ion channels which are thought to be involved in a variety of cellular functions, including cell proliferation, as well as in processes associated with programmed cell death (Connor *et al.*, 1988; Liepins

and Bustamante, 1994; Laniado *et al.*, 1997; Sandström *et al.*, 1994).

Voltage dependent K^+ channels are present in most mammalian cells and voltage dependent inactivating K^+ channels have been described and characterised in primary cultures of rat prostate epithelial cells (Skyrma *et al.*, 1997; Skyrma *et al.*, 1999; Ouadid-Ahidouch *et al.*, 1999). K^+ activity has been implicated in T-lymphocyte activation as well as in the delivery of 'lethal hit' by cytotoxic T-lymphocytes and in tumour cells undergoing T cell-mediated lysis (Bregetowski, 1986). Activation of K^+ channels results in an efflux of K^+ with a net decrease of intracellular K^+ , as well as an imbalance in other ions such as Na^+ and Mg^{2+} (Smith *et al.*, 1998; Liepins and Bustamante, 1994; Berger and Garnier, 1999). In addition, it has been suggested that K^+ channel function may also be required for tumour cell surface vesicle formation and shedding, changes in membrane permeability and nuclear fragmentation, i.e., the events leading to what we know by the term 'programmed cell death' (Gutierrez *et al.*, 1999). Prevention of etoposide induced apoptosis in thymocytes by blockage of K^+ channels has recently been reported (Dallaporta *et al.*, 1999).

Our results with PC-3 cells after etoposide treatment reveal a progressive decrease of intracellular K^+ , as cells pass from the first to second stage of induced apoptosis, and a dramatic lowering in the third stage. We also noticed that the morphology of the cells was changing: cells in the second stage become ruffled and blebbed, as intracellular Na^+ and Mg^{2+} increase and K^+ decreases. The cell membrane permeability at this stage remains unaltered as we could demonstrate by dye exclusion assays. The ionic ratios are also indicative of an adequate function of the Na^+/K^+ pump. A progressive increase in Na^+/K^+ ratio compatible with cell injury as cells progress through the stages of apoptosis finally shows values which can be considered as a sign of severe cell damage (Skepper *et al.*, 1999; Fernandez Segura *et al.*, 1999; Orlov *et al.*, 1999; Kampf *et al.*, 1999). The reduced levels of potassium together with the high sodium and chloride levels found in those cells after etoposide treatment, may be connected to an impairment of the Na^+/K^+ pump, related to cell damage. By this time, cells have reached the third phase of the process, and the cell membrane is now permeable to vital dyes.

The positive correlation between the levels of calcium and phosphorus in the third phase of the process, indicates the possibility that high local calcium concentrations could be due to deposition

of calcium phosphate. Control cells appeared to have the characteristic elemental pattern of viable cells, with low Na^+ and high K^+ , Mg^{2+} and P during the assay (Grängsjö *et al.*, 1996; Hongpaisan and Roomans, 1995; Roomans, 1988; Roomans, 1990).

Parallel changes in cellular volume were observed. Cells maintain and regulate their volume by controlling intracellular solute concentrations and water flux across the cell membrane (Christensen, 1987; Hazama and Okada, 1990; Shuba *et al.*, 1999; Rothstein and Mack, 1990). The variation in cellular volume was evaluated using the sum of the Na^+ and K^+ content. Apoptotic cells progressively shrank when compared to control cells or to preceding stages of the apoptotic process. Ion fluxes also reveal volume changes with an apparent secretion of chloride accompanied by K^+ efflux (Hazama and Okada, 1988; Hazama and Okada, 1990; Cliff and Frizzell, 1990; Baro *et al.*, 1994; Kwong *et al.*, 1999).

In conclusion, we demonstrate that the use of electron probe X-ray microanalysis makes it possible to evaluate alterations in total element composition in individual cells during apoptosis. We showed that three morphologically identifiable stages of apoptosis are associated with alterations of intracellular ions, mainly sodium, chlorine and potassium, as well as with changes in the phosphorus/sulfur ratio. The use of X-ray microanalysis can, thus, be a helpful tool for further studies on cellular mechanisms involved in the control of programmed cell death of prostatic cancer cells.

REFERENCES

- ABRAHAM EH, BRESLOW JL, EPSTEIN J, CHANG-SING, LECHENE C, 1985. Preparation of individual human diploid fibroblasts and study of ion transport. *Am J Physiol* **248**: C154-164.
- BARBIERO G, DURANTI F, BONELLI G, AMENTA JS, BACCINO FM, 1995. Intracellular ionic variations in the apoptotic death of L cells by inhibitors of cell cycle progression. *Exp Cell Res* **217**: 410-418.
- BARO I, ROCH B, HONGRE AS, ESCANDE D, 1994. Concomitant activation of Cl^- and K^+ currents by secretory stimulation in human epithelial cells. *J Physiol (London)* **478**: 469-482.
- BEAUVAIS F, MICHEL L, DUBERTRET L, 1995. Human eosinophils in culture undergo a striking and rapid shrinkage during apoptosis. *J Leukocyte Biol* **57**: 851-856.
- BENSON RSP, HEER S, DIVE S, WATSON AJM, 1996. Characterization of cell volume loss in CEM-C7A cells during dexamethasone-induced apoptosis. *Am J Physiol* **270**: C1190-C1203.
- BERGER R, GARNIER Y, 1999. Pathophysiology of perinatal brain damage. *Brain Res Brain Res Rev* **30**: 107-134.

- BORGES RR, FURUYA Y, REMINGTON L, ENGLISH HF, JACKS T, ISAACS JT, 1993. Cell proliferation, DNA repair and p53 function are not required for programmed cell death of prostatic glandular cells induced by androgen ablation. *Proc Natl Acad Sci USA* **90**: 8910–8914.
- BORNER MM, MYERS CE, SARTOR O, SEI Y, TOKO T, TREPPEL JB, *et al.*, 1995. Drug induced apoptosis is not necessarily dependent on macromolecular synthesis or proliferation in the p53 negative human prostate cancer cell line PC-3. *Cancer Res* **55**: 2122–2128.
- BOWEN ID, WORRILL NA, WINTERS CA, MULLARKEY K, 1988. The use of backscattered electron imaging, X ray microanalysis and x-ray microscopy in demonstrating physiological cell death. *Scanning Microsc* **2**: 1453–1462.
- BREGETOWSKI P, REDKOZUBOV A, ALEXEEV A, 1986. Elevation of intracellular calcium reduces voltage-dependent potassium conductance in human T cells. *Nature* **319**: 776–778.
- CHRISTENSEN O, 1987. Mediation of cell volume regulation by Ca^{2+} influx through stretch-activated channels. *Nature* **330**: 66–68.
- CLIFF WH, FRIZZELL RA, 1990. Separate Cl^- conductances activated by cAMP and Ca^{2+} in Cl^- secreting epithelial cells. *Proc Natl Acad Sci USA* **87**: 4956–4960.
- CONNOR J, SAWCZUK IS, BENSON MC, TOMASHEFSKY P, O'TOOLE KM, OLSSON CA, BUTTYAN R, 1988. Calcium channel antagonists delay regression of androgen-dependent tissues and suppress gene activity associated with cell death. *Prostate* **13**: 119–130.
- DALLAPORTA B, HIRSCH T, SUSIN SA, ZAMZAMI N, LAROCHE N, BRENNER C, MARZO I, KROEMER G, 1998. Potassium leakage during the apoptosis degradation phase. *J Immunol* **160**: 5605–5615.
- DALLAPORTA B, MARCHETTI P, DE PABLO MA, MAISSE C, DUC HT, METIVIER D, ZAMZAMI N, *et al.*, 1999. Plasma membrane potential in thymocyte apoptosis. *J Immunol* **162**: 6534–6542.
- DENMEADE SR, ISAACS JT, 1996. Activation of programmed (apoptotic) cell death for the treatment of prostate cancer. In: August JT, Anders MW, Murad F, Coyle JT, eds. *Advances in Pharmacology*. San Diego, Academic Press. 281–306.
- EARNSHAW WC, 1995. Nuclear changes in apoptosis. *Curr Opin Cell Biol* **7**: 337–343.
- ELDER HY, WILSON SM, JOHNSON AD, 1998. Preparation methods for quantitative x-ray microanalysis of intracellular elements in ultrathin sections for transmission electron microscopy: the freeze dried, resin embedded route. In: *Cell Biology: a laboratory handbook*. Vol. 3, 2nd ed. New York, Academic Press.
- FERNANDEZ-SEGURA E, CAIZARES FJ, CUBERO MA, WARLEY A, CAMPOS A, 1999. Changes in elemental content during apoptotic death studied by electron probe x-ray microanalysis. *Exp Cell Res* **253**: 454–462.
- FROST PJ, BELLDEGRUN A, BONAVIDA B, 1999. Sensitization of immunoresistant prostate carcinoma cell lines to fas/fas ligand-mediated killing by cytotoxic lymphocytes: independence of de novo protein synthesis. *Prostate* **15**: 20–30.
- FUJII F, KIMURA J, TASE C, 1999. Ca^{2+} activated K^+ current induced by external ATP in PC12 cells. *Clin Exp Pharmacol Physiol* **26**: 39–47.
- FUJITA H, YANAGISHAWA A, ISHIKAWA K, 1997. Suppressive effect of a chloride bicarbonate exchange inhibitor on staurosporine-induced apoptosis of endothelial cells. *Heart Vessels, Suppl* **12**: 84–88.
- FURUYA K, LUNDMO P, SHORT AD, GILL DL, ISAACS JT, 1994. Role of calcium, pH and cell proliferation in the programmed (apoptotic) death of androgen independent cells induced by thapsigargin. *Cancer Res* **54**: 6167–6175.
- GRÄNGSJÖ A, LINDBERG M, ROOMANS GM, 1997. Methods for x-ray microanalysis of epidermis: the effect of local anaesthesia. *J Microsc* **186**: 23–27.
- GSCHWEND JE, 1996. Apoptosis. Principles and importance of programmed cell death for prostatic carcinoma. *Urologe A* **35**: 390–399.
- GUTIERREZ AA, ARIAS JM, GARCIA L, MAS-OLIVA J, GUERRERO-HERNANDEZ A, 1999. Activation of Ca^{2+} permeable cation channel by two different inducers of apoptosis in a human prostatic cancer cell line. *J Physiol (London)* **15**: 95–107.
- HALGUNSET J, TVEDT KE, KOPSTAD G, 1992. Cellular differentiation in prostatic explant cultures: assessed by electron microscopy and x-ray microanalysis. *Prostate* **21**: 41–51.
- HAZAMA A, OKADA Y, 1988. Ca^{2+} sensitivity of volume-regulatory K^+ and Cl^- channels in cultured human epithelial cells. *J Physiol (London)* **402**: 687–702.
- HAZAMA A, OKADA Y, 1990. Biphasic rises in cytosolic free Ca^{++} in association with activation of K^+ and Cl^- conductance during the regulatory volume decrease in cultured human epithelial cells. *Pflügers Arch* **41**: 710–714.
- HONGPAISAN J, ZHANG AL, MÖRK AC, ROOMANS GM, 1996. Use of primary cell cultures and intact isolated glandular epithelia for x-ray microanalysis. *J Microsc* **184**: 22–34.
- HONGPAISAN J, ROOMANS GM, 1995. Use of postmortem and in vitro tissue specimens for x-ray microanalysis. *J Microsc* **180**: 93–105.
- HUGHES FM, BORTNER CD, PURDY GD, CIDLOWSKI JA, 1997. Intracellular K^+ suppresses the activation of apoptosis in lymphocytes. *J Biol Chem* **272**: 30567–30576.
- INGRAM P, SHELBURNE JD, LE FURGEY A, 1999. Principles and instrumentation. In: Ingram P, Shelburne J, Roggli V, Le Furgey A, eds. *Biomedical applications of microprobe analysis*. London, Academic Press. 1–58.
- KAMPF C, RELOVA AJ, SANDLER S, ROOMANS GM, 1999. Effects of TNF alpha, IFN gamma and IL beta on normal human bronchial epithelial cells. *Eur Resp J* **14**: 84–91.
- KAWAMURA K, GRABOWSKI D, KRIVACIC K, HIDAKA H, GANAPATHI R, 1996. Cellular events involved in the sensitization of etoposide resistant cells by inhibitors of calcium-calmodulin-dependent processes. *Biochem Pharmacol* **52**: 1903–1909.
- KERR JFR, WYLLIE HA, CURRIE AR, 1972. Apoptosis: a basic biological phenomenon with wide range implications in tissue kinetics. *Br J Cancer* **26**: 239–257.
- KERR JFR, WINTERFORD CM, HARMON BV, 1994. Apoptosis. Its significance in cancer and cancer therapy. *Cancer* **73**: 2013–2026.
- KWONG J, CHOI HL, HUANG Y, CHANG FL, 1999. Ultrastructural and biochemical observations on the early changes in apoptotic epithelial cells on the rat prostate induced by castration. *Cell Tissue Res* **298**: 123–136.
- KYPRIANOU N, ENGLISH HF, ISAACS JT, 1990. Programmed cell death during regression of PC-82 human prostate cancer following androgen ablation. *Cancer Res* **50**: 3748–3753.
- KYPRIANOU N, 1994. Apoptosis: therapeutic significance in the treatment of androgen-dependent and androgen-independent prostate cancer. *World J Urol* **12**: 299–303.
- LANIADO ME, LLANI EN, FRASER SP, GRIMES JA, BHANGAL G, DJAMGOZ MB, ABEL PD, 1997. Expression and functional analysis of voltage-activated Na^+ channels in human

- prostate cancer cell lines and their contribution to invasion in vitro. *Am J Pathol* **150**: 1213–1221.
- LE FURGEY A, SHELBURNE JD, INGRAM P, 1999. Preparatory techniques, including cryotechnology. In: Ingram P, Shelburne J, Roggli V, Le Furgey A, eds. *Biomedical applications of microprobe analysis*. London, Academic Press. 59–86.
- LIEPINS A, BUSTAMANTE JO, 1994. Cell injury and apoptosis. *Scanning Microsc* **8**: 631–641.
- LU S, TSAI SY, TAI MJ, 1999. Molecular mechanisms of androgen-independent growth of human prostate cancer LNCaP cells. *Endocrinology* **140**: 5054–5059.
- MCCARTHY JV, COTTER TG, 1997. Cell shrinkage and apoptosis: a role for potassium and sodium ion efflux. *Cell Death Differ* **4**: 756–770.
- MCCONKEY D, 1996. The role of calcium in the regulation of apoptosis. *Scanning Microsc* **10**: 777–794.
- ORLOV SN, THORIN-TRESCASES N, KOTELEVTSV SV, TREMBLAY J, HAMEY P, 1999. Inversion of the intracellular Na⁺/K⁺ ratio blocks apoptosis in vascular smooth muscle at a site upstream of caspase-3. *J Biol Chem* **274**: 16545–16552.
- OUADID-AHIDOUCH H, VAN COPPENOLLE F, LE BOURHIS X, BELHAJ A, PREVARSKAYA N, 0000. Potassium channels in rat prostate epithelial cells. *FEBS Letter* **459**: 15–21.
- RODMAN SMITH N, CAMERON IL, 1999. Ionic regulation of proliferation in normal and cancer cells. In: Ingram P, Shelburne J, Roggli V, Le Furgey A, eds. *Biomedical applications of microprobe analysis*. London, Academic Press. 445–460.
- ROOMANS GM, 1988. Quantitative x-ray microanalysis of biological specimens. *J Electron Microscop* **9**: 19–44.
- ROOMANS GM, 1990. X-ray microanalysis. In: Hawkes PW, Valdré U, eds. *Biophysical Electron Microscopy*. London, Academic Press. 347–412.
- ROOMANS GM, 1991. Cryopreparation of tissue for clinical applications of x ray microanalysis. *Scanning Microsc Suppl* **5**: S95–S107.
- ROOMANS GM, VON EULER A, 1996. X-ray microanalysis in cell biology and cell pathology. *Cell Biol Int* **20**: 103–109.
- ROOMANS GM, HONGPAISAN J, JIN Z, MÖRK AC, ZHANG A, 1996. In vitro systems and cultured cells as specimens for x-ray microanalysis. *Scanning Microsc Suppl* **10**: 359–370.
- ROTHSTEIN A, MACK F, 1990. Volume-activated K⁺ and Cl⁻ pathways of dissociated epithelial cells (MDCK): role of Ca²⁺. *Am J Physiol* **258**: 827–834.
- SALIDO M, LOPEZ A, APARICIO J, LARRAN J, VILCHES J, 1996. Etoposide induced apoptosis in prostatic androgen independent cell lines. *Int J Dev Biol Suppl* **1**: 191–192.
- SALIDO M, LARRAN J, LOPEZ A, VILCHES J, APARICIO J, 1999. Etoposide sensitivity of human prostatic cancer cell lines PC-3, Du 145 and LNCaP. *Histol Histopathol* **14**: 125–134.
- SANDSTRÖM PE, JONSSON O, GRANKVIST K, HENRIKSSON R, 1994. Identification of potassium flux pathways and their role in the cytotoxicity of estramustine in human malignant glioma, prostatic carcinoma and pulmonary carcinoma cell lines. *Eur J Cancer* **30**: 1822–1826.
- SARASTE A, 1999. Morphologic criteria and detection of apoptosis. *Herz* **24**: 189–195.
- SCHWARTZ LM, OSBORNE BA, 1993. Programmed cell death, apoptosis and killer genes. *Immunol Today* **14**: 582–590.
- SCHWARTZMAN RA, CIDLOWSKI JA, 1993. Apoptosis: the biochemistry and molecular biology of programmed cell death. *Endocrine Rev* **14**: 133–151.
- SKEPPER JN, KARYDIS I, GARNETT MR, HEGYL L, HARDWICK SJ, WARLEY A, MITCHINSON MJ, et al., 1999. Changes in elemental concentrations are associated with early stages of apoptosis in human monocyte-macrophages exposed to oxidized low-density lipoprotein: an x-ray microanalytical study. *J Pathol* **188**: 100–106.
- SKRYMA RN, PREVARSKAYA NB, DUFY-BARBE L, ODESSA MF, AUDIN J, DUFY B, 1997. Potassium conductance in the androgen-sensitive prostate cancer cell line, LNCaP: involvement in cell proliferation. *Prostate* **33**: 112–122.
- SKRYMA R, VAN COPPENOLLE F, DUFY-BARBE L, DUFY B, PREVARSKAYA N, 1999. Characterization of Ca²⁺ inhibited potassium channels in the LNCaP human prostate cancer cell line. *Receptors Channels* **6**: 241–253.
- SHUBA IM, SKRYMA RN, PREVARSKAYA NB, 1999. Volume sensitive anion conductivity in a human prostatic carcinoma cell line. *Fiziol Zh* **45**: 27–34.
- SZABO I, LEPPEL-WIENHUES A, KABA, ZORATTI M, GULBINS E, LANG F, 1998. Tyrosin-kinase-dependent activation of a chloride channel in CD95-induced apoptosis in T lymphocytes. *Proc Natl Acad Sci USA* **95**: 6169–6174.
- SMITH P, RHODES NP, SHORTLAND AP, FRASER SP, DJAMGOZ MB, KE Y, FOSTER CS, 1998. Sodium channel protein expression enhances the invasiveness of rat and human prostate cancer cells. *FEBS Letters* **423**: 19–24.
- TU H, JACOBS SC, BROKOWSKI A, KIPRIANOU N, 1996. Incidence of apoptosis and cell proliferation in prostate cancer. Relationship with TGF-beta and bcl-2 expression. *Int J Cancer (Pred Oncol)* **69**: 357–363.
- WARLEY A, 1990. Standards for the application of X-ray microanalysis to biological specimens. *J Microsc* **134**: 327–333.
- WARLEY A, 1997. *X-Ray Microanalysis for biologists*. Cambridge, Portland Press.
- ZHU N, WANG Z, 1999. Calreticulin expression is associated with androgen regulation of the sensitivity to calcium ionophore-induced apoptosis in LNCaP prostate cancer cells. *Cancer Res* **59**: 1896–1902.